

The energy source of the filaments around the giant galaxy NGC 1275

A.C. Fabian^{1*}, J.S. Sanders¹, R.J.R. Williams², A. Lazarian³, G.J. Ferland⁴ and R.M. Johnstone¹

¹ Institute of Astronomy, Madingley Road, Cambridge CB3 0HA

² AWE plc, Aldermaston, Reading RG7 4PR

³ Astronomy Department, University of Wisconsin, Madison, WI 53706, USA

⁴ Department of Physics, University of Kentucky, Lexington, KY 40506, USA

Contains Material (c) Crown Copyright MoD/2011

1 February 2018

ABSTRACT

The brightest galaxy in the nearby Perseus cluster, NGC 1275, is surrounded by a network of filaments. These were first observed through their H α emission but are now known to have a large molecular component with a total mass approaching $10^{11} M_{\odot}$ of gas. The filaments are embedded in hot intracluster gas and stretch over 80 kpc. They have an unusual low excitation spectrum which is well modelled by collisional heating and ionization by secondary electrons. Here we note that the surface radiative flux from the outer filaments is close to the energy flux impacting on them from particles in the hot gas. We propose that the secondary electrons within the cold filaments, which excite the observed submillimetre through UV emission, are due to the hot surrounding gas efficiently penetrating the cold gas through reconnection diffusion. Some of the soft X-ray emission seen from the filaments is then due to charge exchange, although this is insufficient to account for all the observed X-ray flux. The filaments are complex with multiphase gas. Interpenetration of hot and cold gas leads to the filaments growing in mass, at a rate of up to $100 M_{\odot} \text{ yr}^{-1}$. The lack of soft X-ray cooling emission in cool core clusters is then due to the non-radiative cooling of hot gas on mixing with cold gas around and within the central galaxy.

Key words: X-rays: galaxies — galaxies: clusters — intergalactic medium — galaxies: individual (NGC 1275)

1 INTRODUCTION

Networks of filaments are seen surrounding the central galaxy in some cluster of galaxies (Baade & Minkowski 1954; Lynds 1972; Johnstone, Fabian & Nulsen 1987; Heckman et al 1989; Crawford et al 1999). A relatively nearby and spectacular example is the filamentary nebulosity around NGC 1275 at the centre of the Perseus cluster of galaxies. This has been extensively studied with recent images of the bright H α emission being published by Conselice et al (2001) and Fabian et al (2008). The origin and means of excitation of these filaments remain a matter of debate. They are unlikely to be photoionized since the known sources of ionizing radiation are not luminous or distributed enough. The emission spectrum of the filaments is also unlike that of any known Galactic nebula (although it bears comparison with the Crab Nebula). Strong molecular emission is also present (Edge 2001, Edge et al 2002, Donahue et al 2000, Hatch et al 2005) in this and similar brightest cluster

galaxies. H₂ vibration temperatures of several thousand degrees are inferred (Wilman et al 2002; Jaffe et al 2001). CO emission is mapped across the galaxy and even the outer filaments (Salome et al 2008), yielding a total molecular mass for the filament system approaching $10^{11} M_{\odot}$. The photoionization models which come closest to reproducing the spectrum do so with high-energy photons (Crawford & Fabian 1992).

Johnstone et al (2007) used Spitzer and ground-based observations to study characteristics of the H₂ emission seen in these filaments. They found a correlation between level excitation energy and the derived excitation temperature. A follow-up study showed that the collisional heating from ionizing particles could account for this correlation, if a range of heating rates were present (Ferland et al 2008). Agreement to within a factor of two over a wide range of line ratios is good evidence that the model is viable. The optical/IR/radio emission-line spectrum most likely originates in gas that is exposed to ionizing particles (Ferland et al 2009).

There are several possible sources of these ionizing particles including true cosmic rays, relativistic particles produced *in situ*

* E-mail: acf@ast.cam.ac.uk

by MHD phenomena, energetic photoelectrons produced by X-ray photoionization, and penetration by particles originating in the surrounding hot gas. Here we argue that the latter is the most likely energy source, due to the coincidence in the energy flux of hot thermal particles onto the filament and the total atomic and molecular emission from the filament.

To explore and test the mechanism we concentrate on a Northern filament in the Perseus cluster about 10 kpc north of the nucleus. It is clearly resolved in deep Chandra observations which show that it has a width and surface brightness distribution very similar to that of the underlying $H\alpha$ feature seen in the WIYN map by Conselice et al (2001) or the Hubble Space Telescope images of Fabian et al (2008); see Fig. 1 and Sanders & Fabian (2007). In Section 2 we address the energetics and penetration of the hot and cold gases. In Section 3 we present and discuss the Chandra X-ray spectrum of the filament. The X-ray spectrum may be consistent with that expected from charge exchange as the highly ionized intracluster medium recombines in contact with the much colder, and much more neutral gas in the filament. The predicted X-ray flux, is however one to two orders of magnitude too faint to explain the observations. We use a spectrum from the XMM-Newton Reflection Grating Spectrometer (RGS) of the cluster core to show that cool X-ray line emission is indeed present, although that spectrum is of a much larger scale than any single filament. We discuss turbulent diffusive reconnection as a means to allow interpenetration to occur in Section 4. Finally we discuss wider implications of the model.

2 THE ENERGETICS AND PENETRATION OF A COLD FILAMENT BY SURROUNDING HOT GAS

We begin by considering the cold filament to be a fixed surface embedded in a much hotter medium, the intracluster gas, and assume thermal pressure balance across the surface. Thermal conduction has been considered several times for transporting thermal energy from the hot to the cold gas (Böhringer & Fabian 1998; Nipoti & Binney 2005; Sparks et al 2009). The cold and hot faces do not interact via classical thermal conduction, since this would lead to a thick interface many kpc thick (e.g. Böhringer & Fabian 1998) which is not seen in X-ray images of the Perseus cluster (Sanders & Fabian 2007; see also Fig. 1). Chandra observations of the hot gas around the Northern filament of NGC 1275 indicate an electron density of $n_e \sim 0.035 \text{ cm}^{-3}$ and a temperature of about 4 keV right up to the filaments, where the temperature drops to around 1 keV (see Section 3). The interaction between the hot and cold components is therefore much more intimate. Saturated conduction would then be appropriate, with a heat flux given by Cowie & McKee (1977) of $5\phi pc_s$, where $\phi \sim 1$ accounts for the uncertain physics, p is the gas pressure and c_s is the sound speed of the gas. This is about $0.1 \text{ erg cm}^{-2} \text{ s}^{-1}$ for the above gas. Note however that the estimate ignores magnetic fields. It is close however to the energy flux in the sonic limit.

Once in the cold gas phase, the (now) suprathermal particles rapidly lose energy by elastic collisions with free electrons, and by several inelastic processes including excitation, ionization, and dissociation of atoms and molecules (Spitzer & Tomasko 1968; Dalgarno et al 1999). Secondary “knock-on” electrons resulting from the initial collision of the energetic suprathermal particles cool by elastic collisions with cool electrons in (mixing) regions when the electron fraction is greater than a few percent cent. They predominantly cool by inelastic collisions when the ionization fraction is

lower. Cloudy uses numerical fits to the Dalgarno et al results to follow the energy loss, excitation, and ionization/dissociation in detail.

The colder gas has a range of temperatures from around $2 \times 10^4 \text{ K}$ and below with an observed $H\alpha$ flux of $\sim 5 \times 10^{-15} \text{ erg cm}^{-2} \text{ s}^{-1} \text{ arcsec}^{-2}$ (Conselice et al 2001), corresponding to an emitted flux of $7 \times 10^{-4} \text{ erg cm}^{-2} \text{ s}^{-1}$. The total emitted surface flux, including $\text{Ly}\alpha$ in the UV to molecular emission in the IR and submm is likely to be 20 times larger or $\sim 10^{-2} \text{ erg cm}^{-2} \text{ s}^{-1}$. This is interestingly close to that of the impinging thermal particles provided that the excitation efficiency f with which they penetrate and excite the cold gas is of order 0.1.

Magnetic fields must play an important role in maintaining the integrity of the filaments and in supporting them against infall in the cluster potential (Fabian et al 2008). This will also prevent instant penetration of particles.

If the media were laminar then the magnetic field would present a major obstacle for diffusion perpendicular to the magnetic field. The effective mean free path of hot particles perpendicular to the magnetic field would be limited to the Larmor radius of hot particles and, even in the case of the maximal rate of diffusion given by the Bohm rate, it is much lower than for non-magnetized plasmas. However, the natural state of astrophysical fluids is turbulent. The diffusion of turbulent fluids perpendicular to the mean magnetic field is typically many orders higher than the laminar estimates (see Lazarian 2006).

The sources of turbulence in intracluster medium are numerous, for instance they may be related to the instabilities between hot and cold gas (e.g. Begelman & Fabian 1990; Knoll & Brackbill 2002; Matsumoto & Hoshino 2006). Without specifying the source of turbulence, it is natural to assume that, on the size scale we are dealing with, the high Reynolds number plasma is in a turbulent state.

It is important to note that the detailed geometry of a filament is complex. The Northern filaments shown in Fig. 1 (right) is about 1 kpc across and is made of threads which are resolved by HST at about 70 pc diameter. Even these cannot be filled by cold gas since their mean density is $\sim 2 \text{ cm}^{-3}$ (Fabian et al 2008) whereas the CO emitting molecular gas (mostly H_2) is $\sim 10^5 \text{ cm}^{-3}$, indicating a volume filling factor $f_V \sim 10^{-5}$. If we assume that the cold gas occupies many strands of radius r within a thread, which is of radius $R \sim 35 \text{ pc}$, then the area covering fraction, $f_A = f_V(R/r)$. Presumably $f_A > 1$ in order that the heat flux into a thread can match the radiated flux, so $r < 10^{15} \text{ cm}$.

It is beyond the scope of the present work to investigate the details of the microscopic processes involved. Here we motivate reasons why the penetration factor f with which the hotter gas particles penetrate the cold gas may be high. If, as a result, the hot particles reach the magnetic field lines which penetrate the cold gas then this will allow them to generate enhanced emission by the processes modelled by Ferland et al (2009). The radiative efficiency of the cold gas is so high (with cooling times very much less than that of the hot gas) that we can largely ignore evaporation of the cold gas (but see Section 3.2.2), which must be slowly accreting mass from the hot phase.

3 THE X-RAY SPECTRUM AND OPTICAL SURFACE BRIGHTNESS OF THE NORTHERN FILAMENT

We now examine the X-ray emission from the filaments, using the Chandra spectrum of the Northern filament (shown in Fig. 2). The

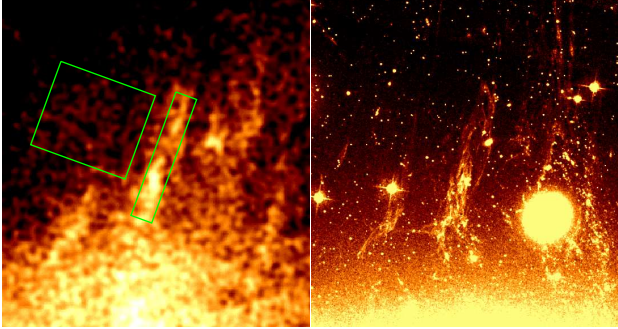


Figure 1. Chandra image of the Northern filament from which the spectrum is measured (right). The long box is 4.1×24.3 arcsec (1.5×9 kpc). The base of it is about 24.4 kpc from the nucleus of NGC 1275.

region is 4.1×24.3 arcsec and background has been subtracted using the neighbouring region shown in the Figure. The spectrum is well fit ($\chi^2 = 332/364$) by a two temperature model with components at $0.66^{+0.07}_{-0.13}$ keV and 1.46 ± 0.26 keV. The abundance of the metals is $0.41^{+0.29}_{-0.15}$ (all uncertainties are at the 90 per cent confidence level). The spectrum is dominated by line emission: we still obtain an acceptable fit ($\chi^2 = 367/364$) if the abundance is raised to 10, indicating that the evidence for any X-ray continuum in the filaments is weak. As shown in Sanders & Fabian (2007), the width of the filament is very similar in the X-ray and visible bands.

The use of a two temperature model does not necessarily mean that all the material present is exactly at the temperatures included. It is perhaps more realistic to assume that there is a continuous range of temperatures leading to emission lines from Si XII to Fe XVII. To check which lines are present, we have examined the XMM RGS data from the core of the cluster.

3.1 The XMM-Newton RGS spectrum of the Perseus cluster core

The RGS data is from a slitless spectrometer with an aperture of 1×4 arcmin. This is much too large to examine any particular region like the Northern filament in detail, but the resultant spectrum again demonstrates that the main features in the spectrum, apart from a bremsstrahlung continuum and a significant contribution from the jetted nucleus, are the expected emission lines. These include Fe XVII which generally indicates emission from gas at ~ 0.5 keV.

We conclude from the Chandra spectrum of the filament that the X-ray spectrum is dominated by emission lines, particularly from Fe-L and oxygen.

3.2 The energetics of filament X-ray emission

3.2.1 Thermal emission from hot gas

In an earlier analysis involving a single temperature for the X-ray cooler gas, Sanders & Fabian (2007) deduced that the filament X-ray emission can be produced by a sheath of 0.7 keV gas with depth ~ 10 pc. This could be the consequence of the mixing of some of the hotter gas with the cold filament gas, but there is no obvious reason for obtaining that intermediate temperature. A mixing layer predicts (Begelman & Fabian 1990) gas an order of magnitude cooler at the geometric mean of the outer, hotter and inner, cooler temperatures (i.e. below 10^6 K). The microphysics of such a

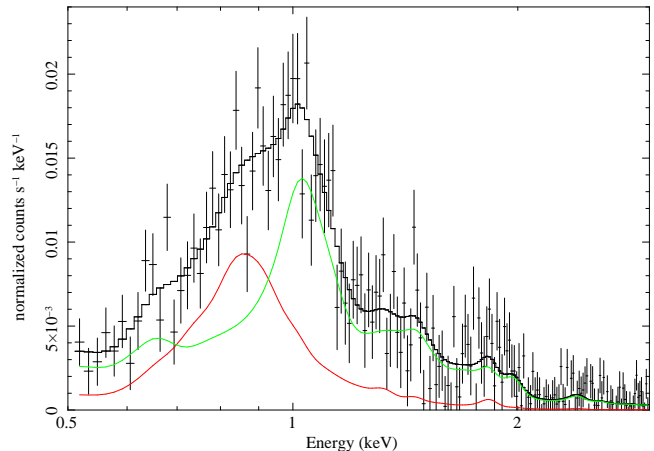


Figure 2. Top: Chandra spectrum of the filament region shown in Fig.1. Background has been subtracted. Bottom: Model of two temperature fit shown in Fig.2

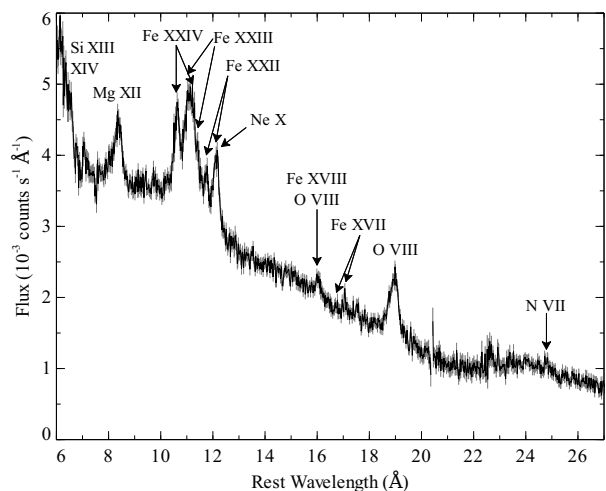


Figure 3. XMM-Newton RGS spectrum of the large region covering the cluster core.

layer is however very complex and beyond detailed consideration here. Instead we consider other processes which may be relevant.

3.2.2 A simple approach to charge exchange emission

We now examine what we expect to observe from hot ionized gas penetrating and mixing with cold neutral gas. The process of charge exchange will dominate with electrons from the neutral gas transferring into excited levels of the impinging ions. The subsequent cascade will result in X-ray line emission. This process is observed in other environments. For example, it explains the X-ray emission from comets seen in our Solar System. Highly-charged ionic species in the Solar Wind interact with the hydrogen halo surrounding a comet to produce a rich and luminous X-ray spectrum (Dennerl et al 1997). The process also causes emission from Jupiter and other planets (e.g. Branduardi-Raymont et al 2007) and from the interaction at the heliosphere and has even been suggested for intracluster filaments (Lallement 2004).

To estimate the energetics in a simple manner for the situation of a cold filament embedded in the hot intracluster medium, we assume that each ion recombines successively, thereby releasing X-

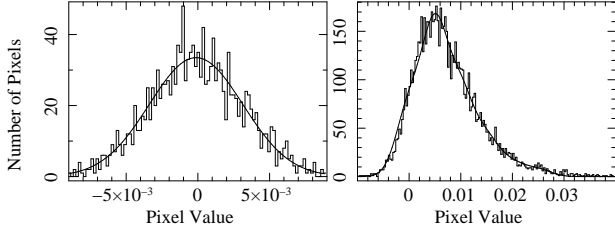


Figure 4. Distribution of pixel values (arbitrary units) in HST F625W optical image for a background region (left) and the Northern Filament (right). A model consisting of a 6 gaussians has been fitted on the right; the standard deviation of each is fixed to be the same as for the background and the pixel value of each steps in equal increments of 5×10^{-3} from 0.

ray photons. The main components are iron which leads to 8 L-shell lines in the 0.7–1.2 keV band and oxygen which lead to two. Multiplying by the relative abundances of iron and oxygen (4.7×10^{-5} and 8.5×10^{-4} relative to hydrogen by number), and assuming their lines emerge around 1 keV on average gives us a fraction of the energy flux of 5×10^{-4} , or a flux of $5 \times 10^{-5} \text{ erg cm}^{-2} \text{ s}^{-1}$, which is ten per cent of the $\text{H}\alpha$ flux of $7 \times 10^{-4} \text{ erg cm}^{-2} \text{ s}^{-1}$. The observed soft X-ray flux is similar to the $\text{H}\alpha$ flux in the Northern filament (Sanders & Fabian 2007). The X-ray flux from simple charge exchange fails by a further factor of two to three when the observed metallicity of the gas ($Z \sim 0.5$) and precise line energies are considered.

Charge exchange predicts soft X-ray emission in the band where emission is observed, but in its simplest form fails by a factor of one to two orders of magnitude (but see discussion in Section 5). The contribution of charge exchange may eventually be discerned with high spectral resolution spectroscopy, since there are characteristic spectral differences from recombination (e.g. Brown et al 2009), including a lack of a continuum.

It is possible that the X-ray emission is thermal and due to mixing of the hot and cold phases resulting in gas at 7–15 million degrees in the space between strands. Additional gas at a warm temperature of around $5 \times 10^5 \text{ K}$ is implied by the detection of OVI emission (Bregman et al 2006) from an aperture covering the central 6.2 kpc of NGC 1275. The filament is therefore highly multiphase, with components ranging from 50 to 10^7 K .

3.3 The optical line surface brightness of filaments

We have investigated the surface brightness distribution in the emission-line filaments using the HST ACS images in the F625W filter published by Fabian et al (2008). These images are particularly sensitive to emission from the $\text{H}\alpha$ and [NII] doublet. The [SII] $\lambda\lambda 6717, 6735$ doublet also lies within the bandpass of the filter but is rather fainter. The filter also transmits continuum light from the galaxy.

We first subtracted a heavily smoothed copy of the F625W image from the unsmoothed data in order to remove the varying background due to the continuum light from NGC 1275. The signal-to-noise ratio of individual pixels is about 2 and we investigate the surface brightness distribution of pixels as follows:

The ds9 interface to Ftools was used to make histograms of the number of pixels with different pixel values at various locations in the nebula. Inspection of these histograms shows that there seems to be a minimum surface brightness for the filaments, well above the background noise level that occurs at a similar level throughout the outer nebula. A region with no filaments present shows an ap-

proximately gaussian histogram centred around zero with standard deviation $\sigma = 3.27 \times 10^{-3}$ (Fig. 4, left).

Data were extracted from a region of the Northern Filament, close to that shown in Fig. 1. The resulting histogram (Fig. 4, right) can be well fit using the sum of 6 gaussian functions. The first gaussian is constrained to the parameters of the background, as measured above. The subsequent gaussians are constrained to have the same width as the background (presumed to be counting statistics) but with centroids corresponding to integer multiples of a minimum intensity value measured somewhere in the nebula.

Although we caution that the fitted model is not unique, a ready interpretation is that the surface brightness of individual filaments is constant while the variation of surface brightness that we observe in the image is due to the superposition of filaments (or strands). The model assumes that all filaments are at the same inclination to the observer, which may be reasonable for the Northern Filament. Our fit, shown as the solid line in Fig. 4 suggests a decreasing trend in the sense for each increase in the number of overlapping filaments there are approximately half as many pixels (or half the area). We conclude that the data are consistent with a roughly constant surface brightness for the threads, as expected by our model.

4 THE RECONNECTION DIFFUSION PROCESS

The interpenetration of hot plasma into filaments can occur through the process of reconnection diffusion (Lazarian et al. 2010, Lazarian 2011). The process is easy to understand. In a laminar fluid magnetic field lines maintain their identity and therefore particles entrained on magnetic field lines stay there indefinitely, provided that Ohmic resistivity is infinitely small. In a turbulent fluid, magnetic fields are being driven perpendicular to their direction and cross each other. A model of reconnection in Lazarian & Vishniac (1999, henceforth LV99) describes the process and shows how the reconnection can be fast, i.e. independent of resistivity. As the LV99 predictions were successfully tested in Kowal et al. (2009), it is sensible to discuss the implications of the model for the filaments we deal with in the paper.

Magnetic field lines from the hot region connect with magnetic fields from the cold region as reconnection proceeds and therefore the hot plasma intermingles with cold material. The excitation of emission in this situation is mediated by reconnection which allows plasma percolation into filaments, but its magnetic energy is not lost via the process. The emission from filaments is only limited by the flow of the hot gas around the filaments and the presence of turbulence which induces fast reconnection and turbulent transport of magnetic field and matter.

It is natural to assume that the turbulent velocity in filaments is less than the Alfvén speed v_A . (In the opposite limit one expects the turbulence to be super-Alfvénic and mix up magnetic fields on the eddy turnover time scale, preventing the existence of long-lived filaments.) The diffusion coefficient for turbulent transport of plasma was estimated in Lazarian (2006):

$$\kappa_{\text{dyn}} \approx L v_L M_A^3 \quad (1)$$

where L is the turbulence injection scale, v_L is the turbulent velocity at injection, $M_A \equiv v_L/v_A$ is the Alfvénic Mach number. The diffusion coefficient given by Eq. (1) is applicable assuming that the size of the diffusion region $r \gg L$. If the radius of filaments is smaller than L , the diffusion coefficient is modified to $\kappa_{\text{dyn}} \approx r v_A (r/L M_A^3)^{1/3}$, provided that $r < L M_A^3$.

The timescale for hot plasma to percolate into a filament of radius r is $\sim r^2/\kappa_{\text{dyn}}$. In the case of $r \sim L$, the time scale of plasma percolation is $\sim M_A^{-3} r/v_L$. These are the timescales over which the plasma and cold gas mix. The flow of plasma into the cold gas can be estimated as $nkTv_{\text{dt}}$, where $v_{\text{dt}} \approx \kappa_{\text{dyn}}/r$.

We note that the linewidths of the filament emission are observed to be moderately high (about 100 km s^{-1} for the outer filaments around NGC 1275, Hatch et al 2006). This is indicative of turbulence in the filaments. The same observations show that the mean velocity field of the filaments is fairly ordered, suggesting that the turbulence is relatively small scale, of the order of the width of a filament.

The process that will compete with the reconnection diffusion is the streaming of hot electrons along magnetic field lines. In any turbulent magnetic field the diffusion of particles along magnetic field lines is different from diffusion along laminar magnetic field lines. The estimate in Lazarian (2006) provides for the diffusion of electrons¹:

$$\kappa_e \approx \frac{1}{3} v_e \lambda M_A^4 \quad (2)$$

where v_e and λ are the velocity and the mean free path of an electron. The mean free path of electrons $\lambda = 300T_3^2 n_{-2}^{-1} \text{ pc}$, where $T_3 \equiv kT/(3 \text{ keV})$ and $n_{-2} \equiv n/(10^{-2} \text{ cm}^{-3})$. The corresponding diffusion velocity of hot electrons into filaments $v_{\text{de}} \approx r/\kappa_e$ is lower than v_{dt} for the numbers adopted².

In summary, turbulent diffusion in which reconnection allows the hot and cold plasma to intermingle can plausibly operate at the hot / cold interfaces. The flow velocity is subAlfvénic in the cold gas or just a few km s^{-1} (the Alfvén velocity in the cold to warm gas is 1 to 10 km s^{-1} if the magnetic field is close to being in pressure equilibrium with the external hot thermal gas). At first sight this does not match the velocity required by the arguments in Section 2, where the flow velocity has to approach the sound speed c_s in the hot gas ($300 - 700 \text{ km s}^{-1}$) to yield a filament flux $\sim pc_s$. However, lack of velocity can be compensated for by increase in surface area. We have argued that a filament is formed of many smaller thread and strand-like components, which means that the total area of the hot–cold interface within a filament is much larger than that presented superficially to an outside observer. We require a factor of 100 to 1000 increase which does not seem unreasonable. There is of course an upper limit to how much flux is obtained from a filament due to the energy flux in the external hot gas, which is of the order of the saturated conduction flux of Cowie & McKee, introduced in Section 2. The observations show that the filaments around NGC 1275 are within a factor of ten of that limit. The observed optical linewidths are probably due to the spread in bulk velocities of the threads and strands within a filament.

Further work is required to identify what keeps the filaments stable, of similar size and presumably similar internal thready structure.

5 DISCUSSION AND CONCLUSIONS

We have shown that there is a fair coincidence between the particle flux impinging on the cold filaments and the total radiation flux emitted by them, as inferred from the observed $H\alpha$ line emission. This provides good evidence that the secondary “knock-on” particles which account for the observed line spectrum from the filaments (Ferland et al 2009) originate from the interpenetration of the hot intracluster gas with the cold filaments.

Turbulent diffusive reconnection provides a reasonable explanation for overcoming the magnetic barrier which would otherwise keep the hot and cold gasses separate. Within the model of reconnection diffusion adopted in the paper magnetic reconnection enables plasma initially entrained on different field lines to come into contact. In other words, magnetic reconnection in turbulent media removes magnetic barriers otherwise existing between hot and cold gas. Alfvénic turbulence inducing motions perpendicular to magnetic field and electrons streaming along wandering magnetic field lines acts to induce efficient thermal conductivity.

Any fast magnetic reconnection process³ dissipates only a small fraction of energy through Ohmic resistivity. The rest goes to straightening magnetic field lines inducing motions of magnetized fluid. This can produce gas heating as well as accelerate energetic particles either through second order Fermi acceleration via the interaction of turbulence in the outflow region with the particles (Larosa & Shore 1998) or through the first order Fermi acceleration as described in De Gouveia dal Pino & Lazarian (2005) (see also Lazarian 2005 and Lazarian et al. 2011). The efficiency of both heating and particle acceleration depend on the amount of free energy that is being released via reconnection. Both theory and numerical simulations (see Goldreich & Sridhar 1995, Lazarian & Vishniac 1999, Cho & Lazarian 2002) testify that magnetic field lines getting more and more parallel to each other with the decrease of the scale of the turbulent motions, thus making less and less energy available to be dissipated via reconnection. In other words, the process of reconnection that we appeal to in this paper does not entail appreciable heating or particle acceleration.

The accompanying X-ray emission is unexplained. The observed X-ray spectrum of the Northern filament appears to be due to Fe-L and O emission lines. The emission could originate in gas at intermediate temperatures ($0.6\text{--}1.5 \text{ keV}$) between the hotter 4 keV gas in which the cold ($T < 5 \times 10^4 \text{ K}$) filaments are embedded, perhaps due to mixing, or evaporation of some strands of cold gas.

Charge exchange is expected to operate however on the highly ionized species interpenetrating the cold gas. We have examined the expected emission from this, which would indeed be Fe-L and O lines emission, but find that the predicted flux fails by a factor of 30, so is too faint to account for the observations. This estimate is based on each incoming ion having only one chance of charge exchange per ion stage. If, as we have argued above, the cold threads are full of tiny strands, it is plausible that an ion might partially recombine when traversing a cold region and then undergo collisional ionization if it then passes into hot gas again. The collisional ionization timescale is only a few per cent of the crossing time of

¹ This is probably an overestimate, as the electric field should prevent free streaming of electrons.

² The reasons why the actual λ may be substantially smaller than our estimate for the mean free path are provided in Lazarian et al. (2011; see also Brunetti & Lazarian 2011). This can only strengthen our conclusion that reconnection diffusion is the dominant source of injecting plasma into filaments.

³ Reconnection is fast when it does not depend on resistivity. In the Lazarian & Vishniac (1999) model of magnetic reconnection, speed is determined by the turbulence injection scale and velocities. These dependences have been confirmed in numerical study by Kowal et al. (2009). Reconnection processes that depend on resistivity are mostly unimportant for astrophysical circumstances, as the magnetic field changes that they can induce are negligibly small.

a filament. We speculate that this may boost the charge exchange emission to the observed level. (Note that charge exchange is not invoked to explain the optical, or infrared, emission from filaments.)

Interpenetration of the cold gas by hot gas means that there is a flux of $\sim 10^6$ particles $\text{s}^{-1} \text{cm}^{-2}$ into the filaments, assuming the values for the N filament. The radiative cooling times of the cold gas are much shorter than any other relevant times so they imply a significant accretion of mass by the filaments. Scaling with this value from the H α flux of the N filament to the total H α luminosity observed from the filaments of NGC 1275 ($2.5 \times 10^{42} \text{ erg s}^{-1}$; Heckman et al 1989) indicates a total mass accretion/cooling rate of $\dot{M} \sim 100 M_{\odot} \text{ yr}^{-1}$. ($\dot{M} \approx 70 L_{43} T_7^{-1} M_{\odot} \text{ yr}^{-1}$, where the total luminosity of the cold/cool gas (about 10–20 times the H α luminosity) $L = 10^{43} \text{ erg s}^{-1}$ and the surrounding hot gas has a temperature of 10^7 K .) There is therefore a significant cooling flow proceeding in the Perseus cluster, with the soft X-ray stage ($kT \sim 3 \text{ keV}$ and below) being carried out by the interpenetration/mixing of the cold gas by the hot gas (as suggested by Fabian et al 2002 and Soker et al 2004). The “missing soft X-ray luminosity” of cool core clusters is comparable to that which emerges at longer wavelengths through the filaments (Fabian et al 2002). The mass cooling rate can adequately balance the star formation rate over the outer filaments of $20 M_{\odot} \text{ yr}^{-1}$ (Canning et al 2010). The mass of the whole filamentary nebulosity will double in about 1 Gyr. Note that we are not arguing that filaments only operate in the coolest parts of the hot gas but just take hot gas from where they happen to be. There may of course be a tendency for there to be more filaments where the hot gas is coolest.

We shall examine the situation for other emission line nebulae found around brightest cluster galaxies in later work. The processes outlined here should apply generally to cold gas embedded in hot or energetic atmospheres such as found in nearby and distant radio galaxies, Ly α nebulosities found at high redshift, the cores of elliptical galaxies and possible LINERs. They may also be relevant to the H α emission from cold gas observed from galaxies being stripped by the intracluster medium in other clusters (e.g. Sun et al 2008; Yagi et al 2010).

ACKNOWLEDGEMENTS

We thank the referee, Ehud Behar, for helpful comments. ACF thanks the Royal Society for support. GJF acknowledges support from NSF (0908877), NASA (07-ATFP07-0124 and 10-ATP10-0053) and STScI (HST-AR-12125.01). AL acknowledges the support of the NSF Center for Magnetic Self-Organization, NSF grant AST 0808118 and NASA grant NNX09AH78G. This research made use of SAOImage DS9, developed by Smithsonian Astrophysical Observatory.

REFERENCES

- Baade W., Minkowski R., 1954, *ApJ*, 119, 215
 Begelman M.C., Fabian A.C., 1990, *MNRAS*, 244, 26
 Böhringer H., Fabian A.C., 1989, *MNRAS*, 237, 1147
 Branduardi-Raymont G., Bhardwaj A., Elsner R.F., Rodriguez P., 2010, *A&A*, 510, 73
 Bregman J.N., Fabian A.C., Miller E.D., Irwin J.A., 2006, *ApJ*, 642, 746
 Brown G.V., et al 2009, *J.Phys. Conf. Ser.*, 163, 012052
 Brunetti, G., & Lazarian, A. 2011, *MNRAS*, 412, 817
 Canning R.E.A., Fabian A.C., Johnstone R.M., Sanders J.S., Conselice C.J., Crawford C.S., Gallagher J.S., Zweibel E., 2010, *MNRAS*, 405, 115
 Cho, J., & Lazarian, A. 2002, *Physical Review Letters*, 88, 245001
 Crawford C.S., Fabian A.C., 1992, *MNRAS*, 259, 265
 Crawford C.S., Allen, S.W., Ebeling H., Edge A.C., Fabian A.C., 1999, *MNRAS*, 306, 857
 Conselice C.J., Gallagher J.S., Wyse R.F.G., 2001, *ApJ*, 122, 2281
 Cowie L.L., McKee C.F., 1977, *ApJ*, 211, 135
 de Gouveia dal Pino, E. M., & Lazarian, A. 2005, *A&A*, 441, 845
 Dalgarno A., Yan M., Liu W., 1999, *ApJS*, 125, 237
 Dennerl K., Englhauser J., Trümper J., 1997, *Sci*, 277, 1625
 Donahue M., Mack, J., Voit G.M., Sparks W., Elston R., Maloney R., 2000, *ApJ*, 545, 670
 Edge A.C., 2001, *MNRAS*, 328, 762
 Edge A.C., Wilman R.J., Johnstone R.M., Crawford C.S., Fabian A.C., Allen S.W., 2002, *MNRAS*, 337, 49
 Fabian A.C., Allen S.W., Crawford C.S., Johnstone R.M., Morris R.G., Sanders J.S., Schmidt R.W., 2002, *MNRAS*, 332, L50
 Fabian A.C., Johnstone R.M., Sanders J.S., Conselice C.J., Crawford C.S., Gallagher J.S., Zweibel E., 2008, *Nature*, 454, 968
 Ferland G.J., Fabian A.C., Hatch N.A., Johnstone R.M., Porter R.L., van Hoof P.A.M., Williams R.J.R., 2009, *MNRAS*, 392, 1475
 Ferland G.J., Fabian A.C., Hatch N.A., Johnstone R.M., Porter R.L., van Hoof P.A.M., Williams R.J.R., 2008, *MNRAS*, 386, L72
 Goldreich, P., & Sridhar, S. 1995, *ApJ*, 438, 763
 Hatch N., Crawford C.S., Fabian A.C., Johnstone R.M., 2005, *MNRAS*, 358, 765
 Hatch N., Crawford C.S., Johnstone R.M., Fabian A.C., 2006, *MNRAS*, 367, 433
 Heckman T.M., Baum S.A., van Breugel W.J.M., McCarthy P., 1989, *ApJ*, 338, 48
 Jaffe W., Bremer M.N., van der Werf P., 2001, *MNRAS*, 324, 443
 Johnstone R.M., Fabian A.C., Nulsen P.E.J., 1987, *MNRAS*, 224, 75
 Johnstone R.N., Hatch N.A., Ferland G.J., Fabian A.C., Crawford C.S., Wilman R.J., 2007, *MNRAS*, 382, 1246
 Knoll D.A., Brackbill J.U., *PhPl*, 9, 3775
 Kowal G., Lazarian A., Vishniac E.T., Otmianowska-Mazur, K., 2009, *ApJ*, 700, 63
 Lallement R., 2004, *A&A*, 422, 391
 Larosa, T. N., & Shore, S. N. 1998, *ApJ*, 503, 429
 Lazarian A., Vishniac E.T., 1999, *ApJ*, 517, 700
 Lazarian A., 2006, *ApJ*, 645, L25
 Lazarian, A., Santos-Lima, R., & de Gouveia Dal Pino, E. 2010, *Astronomical Society of the Pacific Conference Series*, 429, 113
 Lazarian, A. 2005, *Magnetic Fields in the Universe: From Laboratory and Stars to Primordial Structures.*, 784, 42
 Lazarian, A., Kowal, G., Vishniac, E., & de Gouveia Dal Pino, E. 2011, *PLANSS*, 59, 537
 Lynds R., 1970, *ApJ*, 159, L151
 Matsumoto Y., Hoshino M., 2006, *JGRA*, 1110, 213
 Nipoti C., Binney J., 2004, *MNRAS*, 349, 1509
 Salome P., Combes F., Revaz Y., Edge A.C., Hatch N.A., Fabian A.C., Johnstone R.M., 2008, *A&A*, 484, 317
 Sanders J.S., Fabian A.C., 2007, *MNRAS*, 381, 1381
 Soker N., Blanton E.L., Sarazin C.L., 2004, 422, 445
 Sparks W.B., Pringle J.E., Carswell R., Voit M., Cracraft M., Martin R.G., 2009, *ApJ*, 704, L20
 Spitzer L., Tomasko M.G., 1968, *ApJ*, 152, 971
 Sun M., Donahue M., Roediger E., Nulsen P.E.J., Voit G.M., Sarazin C., Forman W., Jones C., 2010, *ApJ*, 708, 946
 Wilman R.J., Edge A.C., Johnstone R.M., Fabian A.C., Allen S.W., Crawford C.S., 2002, *MNRAS*, 337, 63
 Yagi M., et al 2010, *AJ*, 140, 1814